



CHALMERS

Fatigue Life Prediction of Natural Rubber in Engine Mounts

Master's thesis in Applied Mechanics

WILLIAM STÅHLBERG

MASTER'S THESIS IN APPLIED MECHANICS

Fatigue Life Prediction of Natural Rubber in Engine Mounts

WILLIAM STÅHLBERG

Department of Mechanics and Maritime Sciences
Division of Applied Mechanics
CHALMERS UNIVERSITY OF TECHNOLOGY
Göteborg, Sweden 2018

Fatigue Life Prediction of Natural Rubber in Engine Mounts
WILLIAM STÅHLBERG

© WILLIAM STÅHLBERG, 2018

Master's thesis
Department of Mechanics and Maritime Sciences
Division of Applied Mechanics
Chalmers University of Technology
SE-412 96 Göteborg
Sweden
Telephone: +46 (0)31-772 1000

Chalmers Reproservice
Göteborg, Sweden 2018

ACKNOWLEDGEMENTS

I would like to thank the Powertrain Mount division at Volvo Cars for support and for being incredibly friendly and welcoming. I would especially like to thank my supervisor Daniel Högberg for his continuous input and incredibly motivating enthusiasm, it always made working on the thesis fun. I want to thank Henrik Åkesson for lending his expertise in rubber as well as playing a vital role in shaping the fatigue life toolset.

I also want to show my appreciation toward my supervisor Professor Anders Ekberg at Chalmers University of Technology. His expertise in fatigue theory has been invaluable and his encouragement always leaves me inspired. I also want to thank Knut Andreas Meyes at Chalmers for thorough help in finite deformation theory which was tricky.

Finally, I want to thank my friends and family for their support and understanding throughout the course of the project.

This thesis concludes my Master of Science in Engineering studies in Applied Mechanics.

Gothenburg, July 2018
William Ståhlberg

NOMENCLATURE

Nomenclature

\mathbf{r}	Normal vector
dU	Change in stored mechanical energy
$\varepsilon_{1,\max}$	Peak maximum principal strain
A	Crack area
a	Crack size
N_f	Fatigue life
T	Energy release rate
W	Strain energy density
W_c	Cracking energy density
X	Displacement
CED	Cracking energy density
FE	Finite Element
MRE	Main rubber element
NVH	Noise, vibration and harshness
SED	Strain energy density

CONTENTS

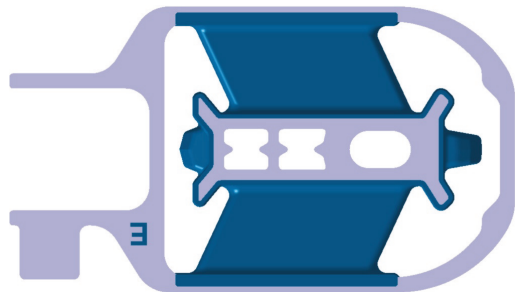
Acknowledgements	i
Nomenclature	iii
Contents	v
1 Introduction	1
1.1 Background	1
1.2 Objectives	2
1.3 Previous work	3
1.4 Limitations	4
2 Literature study	5
2.1 Material properties of rubber	5
2.2 Fatigue analysis of rubber	7
2.3 Propagation of fatigue cracks	10
2.4 Cracking energy density	13
3 Methodology and implementation	15
3.1 Material properties	16
3.2 Numerical implementation of fatigue criteria	17
3.3 Peak maximum principal strain	17
3.4 Cracking energy density	17
3.5 Fatigue failure criterion	20
3.6 Constructing a fatigue relationship	21
3.7 Fatigue life prediction: Variable-amplitude loading	23
3.8 Physical load sequence testing (verification of fatigue life predictions)	24
3.9 The rubber fatigue toolset	25
4 Results	27
4.1 Dependence on hardness and mean strain	27
4.2 Sensitivity to evaluated crack orientations	29
4.3 Sensitivity to fatigue cycle resolution	30
4.4 Sensitivity to removal of fatigue cycles	31
5 Discussion and conclusions	33
5.1 Discussion	33
5.2 Conclusions	34
5.3 Recommendations and future work	34
References	35

1 Introduction

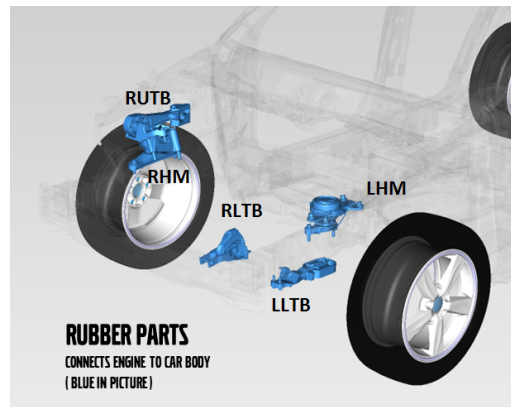
The Master thesis consists of 20 weeks of work, which equals 30 ECTS credits and started January 22nd, 2018 for the Powertrain Mount division of the Volvo Car Corporation. This chapter provides background, objectives and limitations of the work.

1.1 Background

Cars are subjected to many dynamic effects during operation. One such effect is the vibration produced by the internal combustion engine (or electric car motor) during operation. These vibrations transfer to the rest of the car body through the engine mounts or bushings, shown in Figure 1.1. Figure 1.2 shows another typical engine mount in the form of a bushing. As these vibrations are felt by the user, there is a need for these mounts to be able to adequately absorb them. In order to minimize the *noise, vibration and harshness* (NVH) characteristics, it places requirements on the mounts to absorb high-frequency dynamic loads. At the same time, low-frequency engine movements during acceleration and deceleration must be prevented, as they result in an oscillating effect that is also felt by the user, known as *driveability*. Finally, *ride comfort* is affected by how well the mounts handle vertical movements caused by adverse road conditions such as potholes and surface roughness.



(a) A typical engine mount with the rubber portion in blue. From [1].



(b) The four engine mounts are marked in blue [2].

Figure 1.1: The engine is mounted to four engine mounts which serve to absorb vibrations and impact loads.

These three properties lead to contradictory requirements on the stiffness and dynamic response of the engine mounts. Therefore a compromise is made between them. Currently, engine mounts and bushings in Volvo cars are produced and tested by external suppliers. It is however of interest to be able to produce these in-house, as it would greatly reduce lead times and expenses during the iterative component development process. One of the main aspects of designing a mount is the fatigue life. It is therefore a goal to understand the fatigue behavior of the rubber used in these mounts.

When designing an engine mount, the fatigue life of the main rubber element (MRE), denoted (1) in Figure 1.2, is of great interest, as it is the determining factor in the life of the

mount. Cracks often develop at the end of the MRE close to the insert, denoted (3). Natural rubber is used exclusively in engine mounts, due to its superior fatigue resistance compared to synthetic rubbers.



Figure 1.2: A bushing consists of the 1) Main rubber element (MRE), 2) Back snubber/bumpstop, 3) Insert, 4) Front snubber/bumpstop, 5) Outer frame, where the purple and gray colors highlight the rubber and aluminum portions, respectively.

1.2 Objectives

The current reliance on external suppliers results in expensive and time consuming iterations between Volvo Cars and its suppliers. It is a goal to minimize this dependence and reduce lead times and costs by building knowledge and establish a development process for design of powertrain mounts in-house, with the supplier primarily focusing on choice of material. Having a complete control of the development process is known as build-to-print production, illustrated in Figure 1.3. This strive creates the necessity to be able to predict the fatigue life. As part of this project, a methodology of fatigue life prediction was to be developed in Python [3] and MATLAB [4], based on a literature study of current prediction methods. The methodology was to be integrated into a complete fatigue prediction toolset. The commercial fatigue prediction software fe-safe/Rubber was also to be evaluated and the benefit of such software over an in-house method was assessed.

The effect of load representation, mesh dependence, material response, strain crystallization, Mullins effect [1], temperature and reliability was to be assessed, as well as sensitivity studies with respect to implementation variables and load histories. Results from previous research on fatigue of rubber was to be used in evaluating the reliability of the in-house fatigue prediction method. The engine mounts were to be evaluated in Abaqus/Standard [5] and the obtained stress-strain response was to be used to predict the fatigue life. The material stress-response

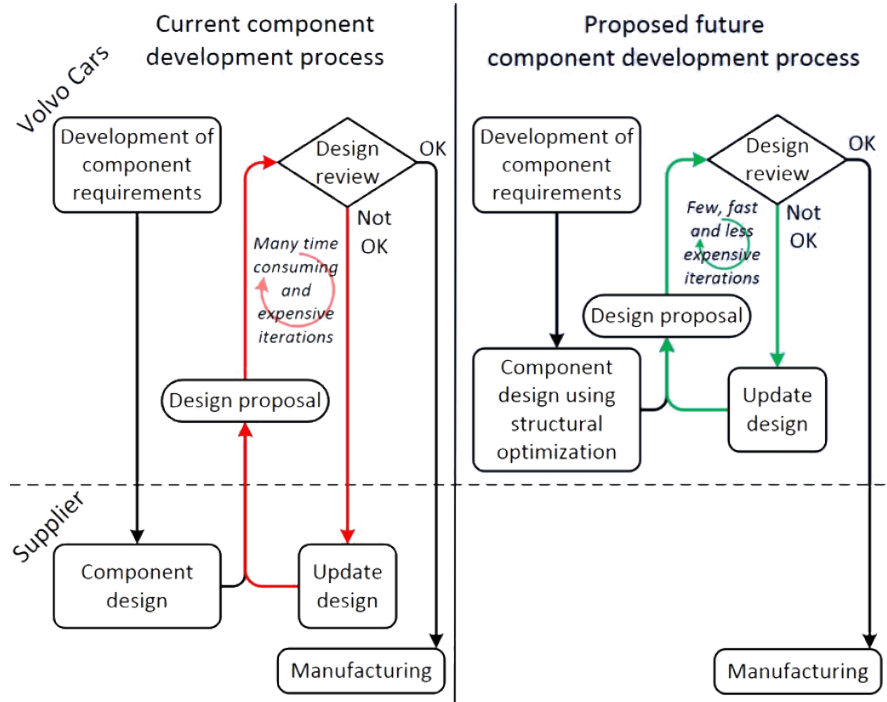


Figure 1.3: *The proposed future development process, known as build-to-print, would mean less reliance on suppliers which reduces lead times and cost. From [1].*

data that was to be used is the same source that is currently in use by the Powertrain Mount division. It is based on data from Austrell [6].

The following objectives are identified:

- Conduct a literature study of current methods of fatigue life prediction of rubber, with a focus on engine mounts.
- Develop an in-house fatigue prediction algorithm in Python and MATLAB.
- Develop a toolbox for processing of fatigue load histories and fatigue life prediction based on the fatigue prediction algorithm and including a way to construct fatigue data.
- Assessment of the need for the fatigue life prediction software fe-safe/Rubber compared to an in-house method.
- Comparison of the in-house method with previous research and analysis of the reliability of the fatigue method.

1.3 Previous work

The effort of developing build-to-print methods has involved three previous Master thesis projects. Öhrn [7] developed a method of modeling the static and dynamic behavior of rubbers, with a focus on a Volvo V40 engine mount by using the overlay material model [6], which yielded a good correlation between simulations and experimental data up to frequencies of 80 Hz and displacements of 4 mm.

Medbo [8] investigated the structural optimization of a tie bar in order to fit a desired force-displacement response. The optimization consisted of designing a principal geometry, morphing points were chosen, an algorithm evaluated the stiffness response and made iterative changes to the geometry in order to better fit the desired response. The work also introduced a proposed future build-to-print development process of structural optimization.

Finally, Sandell [1] performed mechanical testing of four filled natural rubbers of varying hardness that are currently in use in some of the engine mounts, in order to obtain static and dynamic material parameters. The work described the theory and assessed the viability of obtaining rubber material data in-house.

An extensive overview of previous work in fatigue life evaluation of rubbers is presented in Chapter 4 Literature study.

1.4 Limitations

Fatigue life evaluation is a complex subject, with many aspects that influence the life of rubber components not found in metal fatigue. In practice however, many of these phenomena have little influence on life prediction relative to other uncertainties during the design process. They can therefore be neglected with relative safety. The limitations of the project are listed below:

- Simulations were done quasistatically. Therefore, dynamic effects such as the Payne [7] effect, viscoelasticity and elastoplasticity are neglected. These effects were assumed to have negligible effect on fatigue life.
- The Mullins effect [7] was not accounted for. Instead fatigue data from preloaded specimens was used to negate the effect.
- The effect of aging and ozone on fatigue life was not taken into account.
- The temperature dependence of rubber stiffness was neglected. Material data were obtained for room temperature, as the difference at operating temperatures is minimal.
- No hand calculations were done to verify FEA results, as such were not feasible. In addition, the project was limited to the Abaqus software suite and was not reproduced in other software.
- Only natural rubber was analyzed, as it is used almost exclusively in engine mounts because of its superior fatigue properties.
- Mechanical material data and fatigue data were not from the same sources. The analyses use the Shore hardness [7] to match different rubber compositions.
- No fatigue data on current rubber engine mounts was used due to lack of availability. However, fatigue data for rubber components of similar characteristics was available and used.
- When calculating the cracking energy density, the load history is divided into discrete steps which were interpolated linearly as opposed to integrating across the response.
- The project did not verify the fatigue life prediction results with physical tests. Instead they were only compared to results from previous research.

2 Literature study

Rubber is extensively used in engineering applications because of its ductility and ability to withstand large strains without permanent deformation. Its mechanical applications include tires, belts, impact bumpers and bushings [9]. As with all dynamic applications, fatigue endurance becomes an important design factor and engine mounts are no exception. As fatigue life simulations in rubber were done quasistatically, the complexities of the dynamic behavior of rubber were not taken into account. However, for the sake of completeness, the effects will be presented briefly in this chapter.

2.1 Material properties of rubber

Rubber is known for having low stiffness and high elasticity. This stiffness is strain rate dependent, and increases rapidly as the strain rate increases. This is described as rubber being viscoelastic. The bulk modulus to shear modulus ratio is in the order of 1000–2000, which results in rubber often being modeled as incompressible [10]. When rubber is loaded by a strain that is greater than the previous maximum, it experiences an irreversible softening of the stress–strain curve. This is known as the Mullins effect, which creates a hysteresis loop during cyclic stress strain loading. The effect is shown in Figure 2.1, where the reduction in stress can be seen after each cycle. The softening stabilizes rather quickly, and therefore initial conditioning of rubber components is always done before fatigue testing [6]. The viscoelastic and elastoplastic properties of rubber also contribute to the hysteresis effect, which is a source of heat during fatigue testing. Rubber can therefore reach non-negligible temperatures if testing is performed at high strain rates. This always needs to be taken into account.

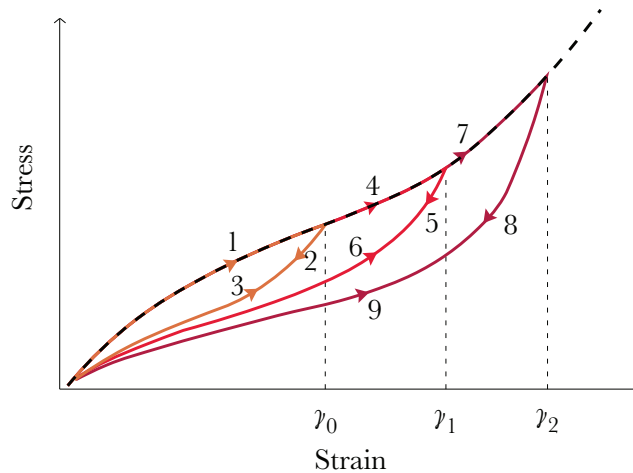


Figure 2.1: *Mullins effect is perceived in virgin rubber that has not been loaded. After each subsequent loading the stress response is reduced. Conditioning involves preloading the specimen 20–100 times [11] at high loads before fatigue testing to eliminate its influence. Adopted from [12].*

When rubber is subjected to an oscillating load, its response can be described by the dynamic

modulus, which includes the static and viscous portion of the material response. Viscoelasticity has previously been modeled in FE software using the overlay model, which makes use of Zener elements [7]. This was not done in this project due to the quasistatic nature of the fatigue simulations. Elastoplasticity, which is modeled using frictional elements [7], was also not considered. The mechanical properties of rubber are temperature dependent. High temperatures reduce the dynamic stiffness and damping. In addition, fatigue life is affected by temperature, with high temperatures reducing life until failure. However, this effect is more pronounced in synthetic rubber than in natural rubbers. In modern internal combustion engines, engine mounts are subjected to temperatures up to 110°C, and in electric cars up to 65°C. Despite not being directly simulated, fatigue testing is always performed at elevated temperatures in order to capture the thermal effects on fatigue life.

The Payne effect [7], also known as the Fletcher-Gent effect, describes the dependence of the viscoelastic storage modulus [13] on the amplitude of the applied strain, see Figure 2.2. The effect causes the storage modulus to decrease when the strain rate is increased. At the same time the damping modulus increases until it reaches a peak, after which it decreases [13]. Recent research [1] has shown that the effect is likely due to reorganization of bonds between the macromolecular matrix and filler structure.

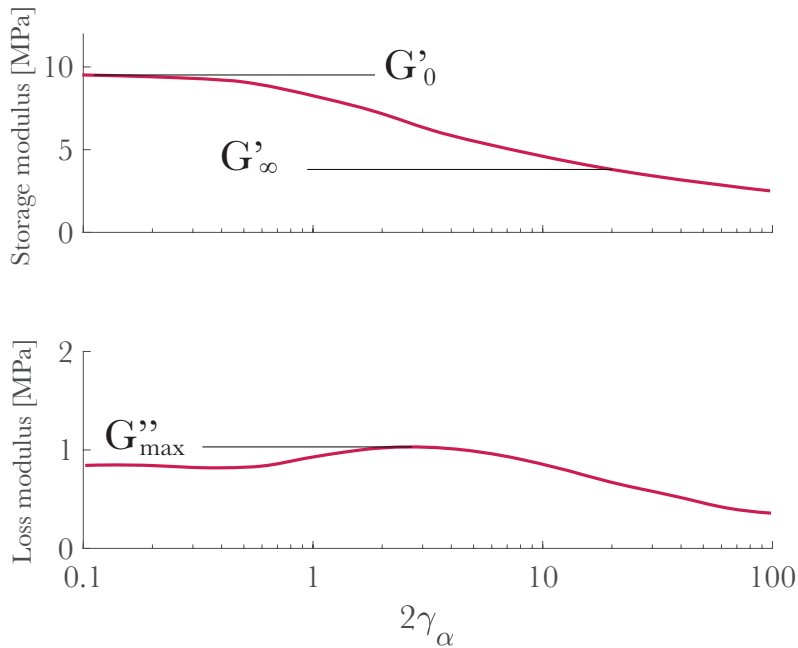


Figure 2.2: *The dependence of the storage and loss moduli [13] on the amplitude of the applied strain. Adopted from [14].*

These effects that have been mentioned are important when modeling the dynamic behavior of rubber, but have a negligible effect on the fatigue life. Strain crystallization is however an effect that is pertinent to fatigue in rubber, and is observed primarily in natural rubbers. As the rubber is stretched, some of the polymer chains in the amorphous material become aligned and produce crystalline structures oriented in the strain direction, as shown in Figure 2.3. These are called lamellae. The crystalline structure acts as a filler in the amorphous

material and greatly increases the tensile strength. This in turn increases the fatigue life. The effect is absent during constant amplitude fatigue testing, but causes fatigue life results of variable amplitude testing to be affected by the order of the load sequence. As an example, if during fatigue testing the highest loads are in the beginning of the test, a longer fatigue life is obtained compared to a test where loads are evenly distributed. This effect is often not taken into account when modeling fatigue damage and can lead to overdimensioning of components.

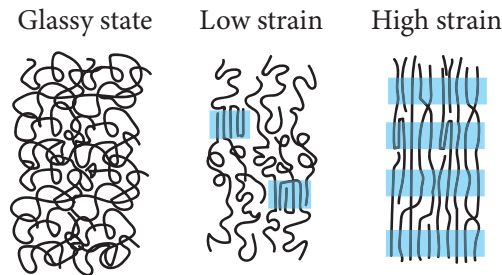
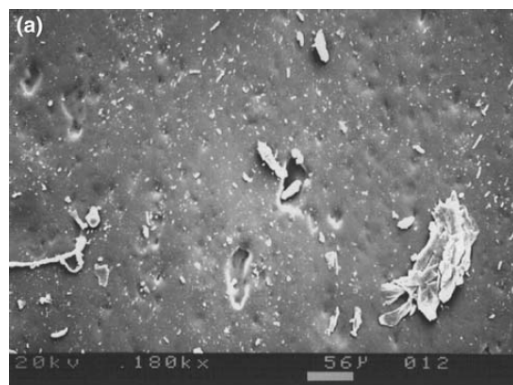


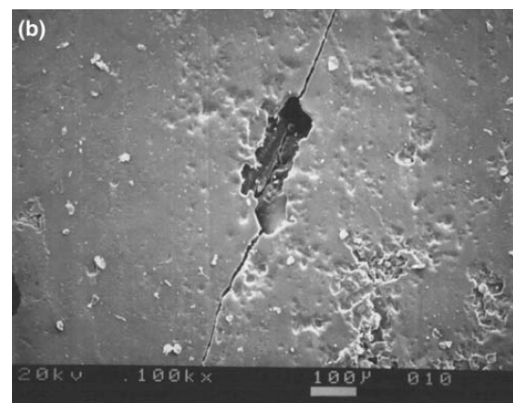
Figure 2.3: As strain is increased, polymer chains become aligned and produce lamellae, crystalline polymer structures. Adopted from [15].

2.2 Fatigue analysis of rubber

Fatigue is the weakening of a material due to cyclic loading. This causes defects in the structure to turn into visible cracks. These cracks grow as the structure continues to be loaded until they reach such a length that the structure experiences sudden fracture. Figure 2.4 features several cracks as seen on the surface of the virgin material. Figure 2.4 b) shows a crack that has developed into a crack after repeated loading.



(a) Virgin rubber surface.



(b) Crack emanating from void on the surface.

Figure 2.4: Crack in rubber initiate from voids and other defects that occur naturally during manufacturing. From [16] and [17].

Fatigue life prediction theory of rubber borrows directly from the mature field of fatigue of metals, although it involves many challenges not related to metals. Many methods that

applied to metals remain valid for rubbers when some modifications are made. The earliest academic study of fatigue was done by Wöhler [18] in the 1860s, motivated by the need to understand fracture of railroad axles. Generally, a fatigue crack is assumed to be small relative to the overall structure of the component throughout its lifetime. Therefore crack initiation becomes the determining factor for the life of a component. This is often true also for rubbers. Commonly, one determines the fatigue life of a component from a scalar parameter, such as the principal stress that a uniaxially loaded bar is subjected to. When components have a complex loading or geometry, one is often required to model it in FE software in order to obtain the stress-strain state. The related fatigue phenomenon is known as multiaxial fatigue. The component is affected by stresses in different directions and a scalar equivalence value that can be related to a fatigue life relationship must be obtained from the stress state. Since a linear stress-strain response is often assumed in metals, it is usually more easy to define. For rubbers on the other hand, the loads at which fatigue becomes an issue are always nonlinear, both in material response and in deformation. In addition, effects like the Mullins effect, Payne effect, strain crystallization, and dynamic damping, can make predicting the stress and in the extension the fatigue response difficult. For this reason, historically fatigue of rubber was measured by using the strain state of the material only [9]. However, this work shows the severe limitations of such an approach.

Two approaches are prevalent in fatigue life theory of rubber. The first assumes an already existing crack with an initial size and predicts the propagation of this crack until it reaches the fracture size. The second is not based on a crack size but rather the loss of stiffness (or loss of function) of a component. In both cases, there are three notable criteria for predicting the life of rubber: the peak principal strain, the strain energy density (SED) and the cracking energy density (CED).

Maximum principal strain is based on research in the 1940s by Cadwell [19] on unfilled natural rubber. A good correlation between the maximum principal strain and fatigue life was found in both tensile and shear loading of rubber. Cadwell also found a property that is unique to natural rubber, which gives it superior fatigue endurance compared to synthetic rubber. When natural rubber is subjected to constant strain amplitudes, the life is improved as the minimum strain is increased. This is because of the unique phenomenon of strain crystallization. Although the peak principal strain yields a good correlation to fatigue life for simple load cases, in the case of more complex loads such as equibiaxial tension, results are less satisfactory.

Strain energy density (SED), developed in the late 50s, proposes that the energy release rate is proportional to the product of SED and the crack size [9]. The conditions for when this is true are however limited, as it turned out to not be as valid for large deformations in complicated geometries where rotations are nonzero. Despite this, much research has gone into the investigation of SED. The strain energy density was even investigated for use in metal fatigue, however correlation of fatigue life was not satisfactory and there were theoretical objections. Despite this, the maximum principal strain and SED remain the most widely used approaches to life estimation in the industry. The reason for this is that the only viable alternative to these two methods, the cracking energy density, is computationally demanding.

In practice, the fatigue life relationships of natural rubber components are obtained on a per-component basis. One develops an empirical relationship between fatigue life and a parameter, such as the maximum principal strain, or by simple rules of thumb that can be used for similar geometries with similar load conditions. Of course, this requires the need for

physical verification, and fatigue life predictions of radically different geometries require new fatigue relationships to be obtained. This is a costly processes that can take up to a year to obtain.

The most fundamental fatigue relationship is the Wöhler curve that relates a parameter describing the cyclic stress–strain state (traditionally the normal stress amplitude) to the number of load cycles that can be endured until failure. A power law can often describe the Wöhler curve well. As an example, Duan [20] performed fatigue testing of engine rubber mounts subjected to loading in a single direction under different temperatures, where the fatigue life N_f was expressed as a function of the maximum principal strain $\varepsilon_{1,\max}$ (at 23°C), as shown in Figure 2.5.

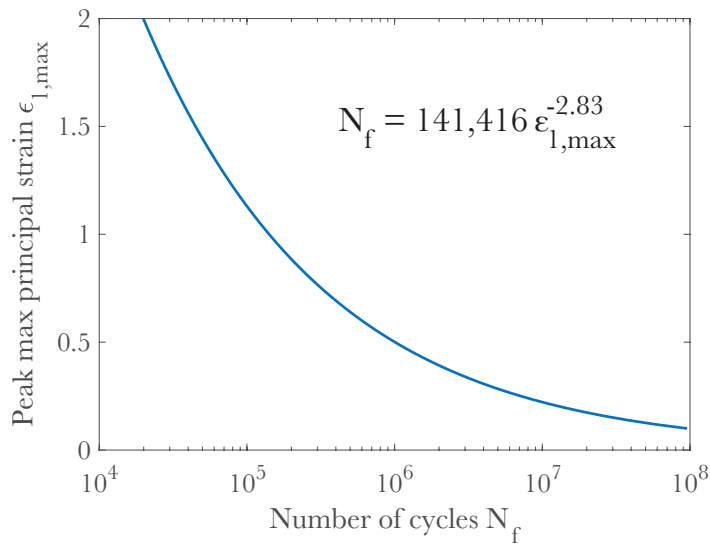


Figure 2.5: *Wöhler curve of fatigue testing of an engine rubber mount subjected to testing at 23°C.*

Another, less geometry-dependent method involves assuming the existence of an initial crack, and integrating the crack growth per cycle up to the fracture size. For natural rubbers it is common to assume an initial crack size in the virgin material to be between 0.01–0.05 mm, as found by Lake [21]. The crack grows until a size is reached where fracture is assumed to be imminent, or where there are relatively few cycles left until failure. This method however requires extensive knowledge of the crack growth characteristics, initial crack size and a well-defined final failure size. It is a common method in fatigue of metals, but in rubbers obtaining this data is often only viable in an academic setting. Furthermore, natural rubber has a tendency to develop networks of fatigue cracks. Translating this network to an equivalent single crack becomes difficult. This is less of a problem with synthetic rubbers which mostly exhibit single well-defined cracks.

In the automotive industry, engine mounts and bushings are exclusively produced in natural rubber and the function of an engine mount is to adhere to a specified force–displacement curve, shown in Figure 2.6. For this reason, fatigue failure is almost exclusively defined as the point at which the static stiffness, or the slope of the force–displacement relationship at $X = 0$,

has been reduced by 20%, see e.g. Woo [22] [23] and Duan [20]. This is the failure criterion used for Volvo mounts and bushings.

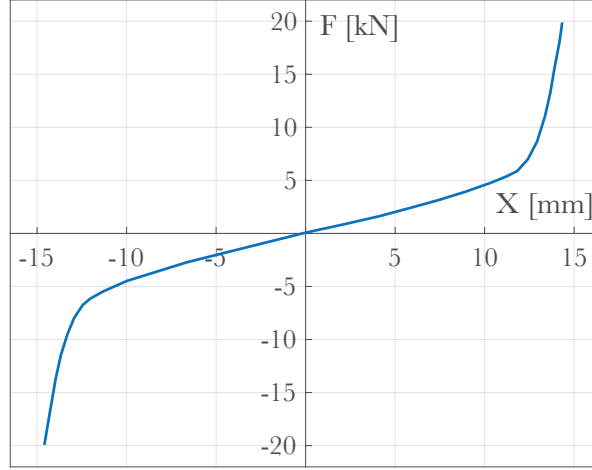


Figure 2.6: *Example of a force–displacement (X) function for mounts and bushings. The static stiffness is defined as the slope of the curve at $X = 0$.*

2.3 Propagation of fatigue cracks

Much research has gone into understanding the evolution of fatigue cracks in rubbers, such as their initiation from voids in the material, the size of these voids, the rate of evolution as a function of energy and crack size, the influence of crack closure, the different patterns of cracks that form depending on load case, the influence of mean strain, aging effects and ozone deterioration effects. Many of the findings will not be discussed in the current work, and are not currently not meaningful enough to be useful in practice. Microscopically, what allows the growth of a crack is the crosslinks between the polymer chains of the rubber structure. These are weak bonds (relative to the polymer chains) and tear apart when subjected to high loads, as illustrated in Figure 2.7. The growth of a fatigue crack is commonly measured as the energy release rate, T . It is a measured of the change in stored mechanical energy dU per unit change in crack area dA [9].

$$T = -\frac{dU}{dA}$$

The energy is denoted T in rubber literature for historical reasons, referring to the tearing energy required under a static load. It was found that during pulsating loading, the crack growth rate is determined by the maximum energy release rate [25]. Examples are the studies by Greensmith in 1963 [26] and further in 1972 by Lindley [27], is that of a single edge cut specimen with a crack of initial size a_0 subjected to tensile loading, as shown in Figure 2.8. The energy release rate was estimated as a function of the strain energy density, W , crack size

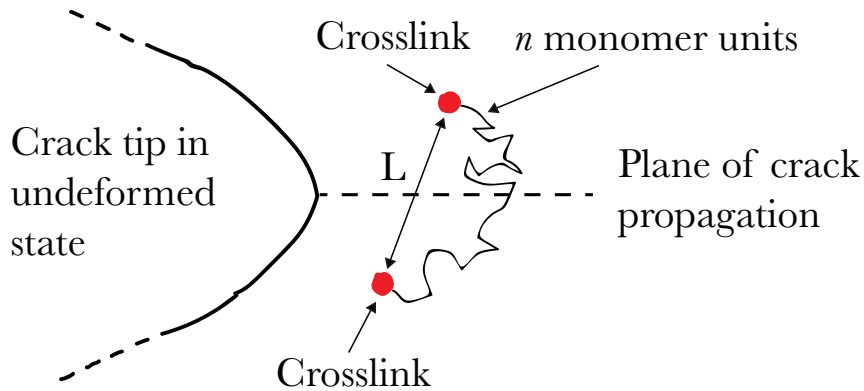


Figure 2.7: *The weak crosslinks between the polymer chains tear apart when subjected to high loads. Adapted from [24].*

a and a coefficient k .

$$T = 2kWa$$

where k is a function of the principal engineering strain:

$$k = \frac{2.95 - 0.08\varepsilon}{(1 + \varepsilon)^{1/2}}$$

if the crack size is small relative to the width of the specimen. In actuality, there are four

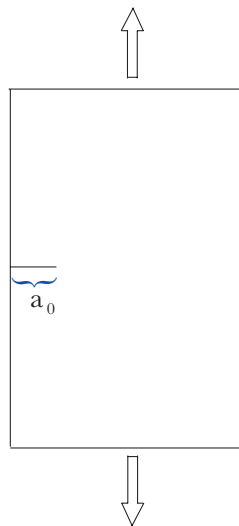


Figure 2.8: *A plate with an initial crack a_0 .*

regimes of fatigue crack growth have been observed in rubbers as shown in Figure 2.9, which shows the crack growth rate \dot{a} and the energy release rate T . In the first regimen, $T < T_0$, the crack growth rate is independent of the energy release rate, T , the rate at which energy

per square unit is dissipated during fracture of the newly created fracture surface area. This means that rubber, unlike metals, has no endurance limit. In rubbers, even the smallest loads cause crack growth, albeit very slow. In the second regime, crack growth follows a linear relationship. In the third regime, crack growth that can be described by a power law and a fourth where the growth rate is infinite (sudden fracture). Several models have been developed to describe the last three regions with one relationship [9]. This is the most common way of estimating life in practical applications, and there is a vast array of research on obtaining power laws based of different geometries and load cases. Despite the multitude of research into

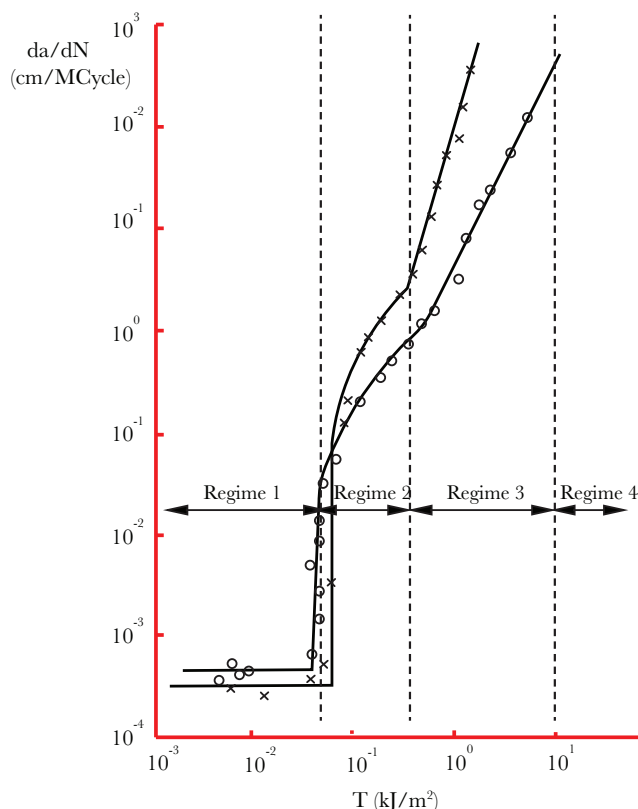


Figure 2.9: *The 4 regimes of crack growth and their relation to the energy release rate. Adopted from [21].*

different approaches to fatigue estimation, no unified method that accounts for the different fatigue effects of rubber has been found. Fatigue relationships are always dependent on the composition and geometry of the test specimen, operating temperature [28], aging [23] and loading sequence order. Strain crystallization is a phenomenon that is specific to natural rubbers, and is a primary reason for its unique superior fatigue resistance. Often this effect is not accounted for, and depending on the load sequence of the fatigue loading, it can lead to overdimensioning or underdimensioning. Strain crystallization occurs during high tensile loading, but the effect can also be experienced during compressive loading, which can have a retarding effect on crack growth rate by crystallization of the crack tip [9]. In concrete terms, for a fatigue test where all of the highest loads are in the beginning of the sequence, the rubber

will reach maximum crystallization, and the remaining lower loads will have less of an effect on crack growth than if the rubber had not been allowed to crystallize. The fatigue life would be overestimated, as in practice load magnitudes are randomly distributed over the lifetime of the component. On the other hand, if the highest loads are relegated to the end of the fatigue testing, the lower loads cause a greater crack growth, and fatigue life will be underestimated.

2.4 Cracking energy density

A model for predicting multiaxial fatigue crack initiation and cracking propagation was proposed by Mars [29] in 2001, motivated by the shortcomings of the previously mentioned approaches. The cracking energy density (CED) is part of the total elastic strain energy density (SED), but focuses on the energy available to a specific material plane during crack growth. This is defined as the increase in energy density as the material is subjected to a fatigue load cycle:

$$dW_c = t_i d\varepsilon_i \quad (2.1)$$

where $t_i = \sigma_{ij}r_j$ is the traction stress on the plane with normal r_j and $d\varepsilon_i = d\varepsilon_{ik}r_k$ is the change in traction strain on the plane. The energy in this plane is the portion of energy available to be released on a material plane [16]. Figure 2.10 shows an example in two dimensions, where the crack plane with the normal, the traction stress and change in strain are shown.

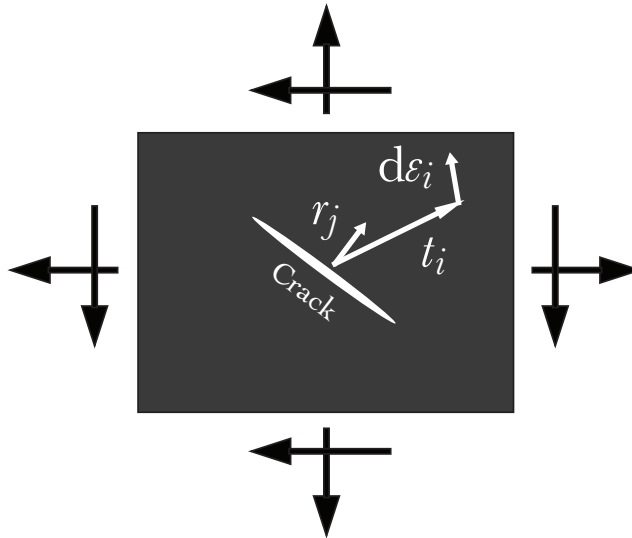


Figure 2.10: A hypothetical crack with orientation \mathbf{r} from which the cracking energy density is calculated. Adapted from [16].

By transforming into principal coordinates, where κ_{jk} is the transformation from the original to the principal coordinate system, one can express the plane normal as $r_j = \kappa_{jk}r_k$. With the principal values σ'_{ij} of the stress σ_{ij} and the principal values $d\varepsilon'_{ik}$ of the strain $d\varepsilon_{ik}$, the cracking energy density can be expressed as

$$W_c = r_l \kappa_{jl} \left(\int_0^{\varepsilon'_{ik}} \sigma_{ij} d\varepsilon_{ik} \right) \kappa_{km} r_m$$

In summary, the classical crack propagation approach assumes a preexisting crack of known location and orientation, which grows until it reaches a failure size a_f . This classical approach, has been difficult to use for rubbers, as the location of crack initiation can be hard to predict if only the principal strain and strain energy density is known. As the function of an engine mount is to conform to a specific force-displacement curve, fatigue failure is defined as the point where the static stiffness has been reduced by 20%. Independent of failure criteria, CED has been shown to be superior to the trivial peak engineering strain as well as the strain energy density. Additionally, CED gives superior results when fitting geometries with complex load histories to a Wöhler curve, as shown by Mars [9] and Harbour [30]. However, CED is computationally expensive. It involves iterating over a finite number of crack orientations in each element of a FE model.

To summarize, the three fatigue evaluation criteria are compared in Table 2.1.

Table 2.1: Comparison of the three common fatigue life prediction parameters.

Maximum principal strain	Strain energy density	Cracking energy density
Easy to obtain	Easy to obtain	Implementation must be developed or purchased
Easy to compute	Easy to compute	High computation times
Only simple load cases	Worst correlation [9]	Complex load cases
Very dependent on material and geometry	Dependent on material and geometry	Less dependent on material and geometry

3 Methodology and implementation

A working implementation of a peak principal strain and CED fatigue life prediction methodology was implemented in MATLAB and Python, using Abaqus as the FEA solver. There are two steps in the process of predicting the fatigue life of a component:

- Constructing a Wöhler curve, which is a relationship between a stress–strain measure and the number of cycles until failure.
- Calculating the damage distribution of the component caused by subjecting it to a varying load sequence that is representative of the lifetime of the component.

The first step is outlined in the diagram in Figure 3.1. Several specimens of a component are subjected to constant-amplitude cyclic loading under different amplitudes until failure, a relationship between the displacement amplitude X and number of cycles N_f is obtained. In order to make the relationship usable for other similar geometries and other materials, the same tests are simulated in FE software. For rubber, a relationship is obtained between the peak maximum principal strain, $\varepsilon_{1,\max}$ or the cracking energy density, W_c , and the number of fatigue cycles until failure. The second step consists of predicting the lifetime of the component

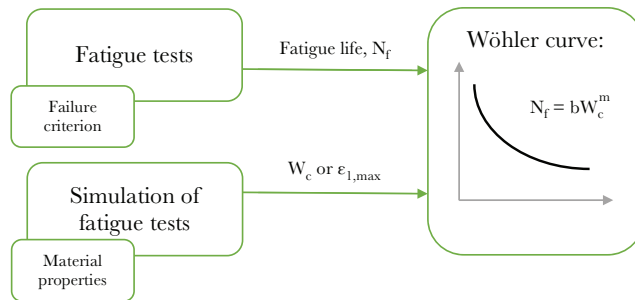


Figure 3.1: *The four steps in fatigue life prediction.*

when it is subjected to operating loads. This is outlined in Figure 3.2. A lifetime load sequence is evaluated and, together with the Wöhler relationship, the damage distribution of the component is obtained. As previously mentioned, a damage above 1 at any material point indicates failure of the component at that material point. The two-step process just described

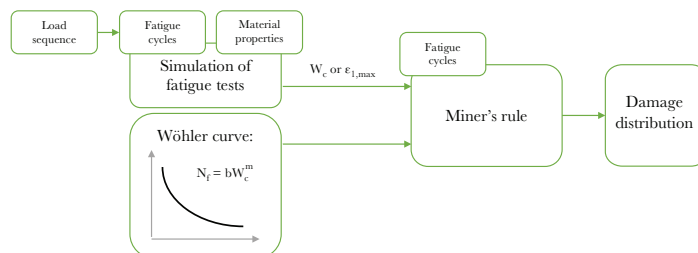


Figure 3.2: *The two steps involved in predicting the fatigue life of a component.*

was implemented, but has not been employed to the analysis of actual components due to time constraints (obtaining the Wöhler relationship commonly takes up to a year). Instead, the sensitivity to parameters and optimal signal and stress–strain resolutions have been assessed.

3.1 Material properties

Before proceeding, the material properties of the component must be determined. The stress response of a material greatly affects the fatigue life, and as such must be chosen with care. One must also be consistent in using the same material model throughout the development of the component.

For the project, the natural rubber was modeled using the hyperelastic energy Yeoh model [1]. An example a Yeoh stress-strain response is shown in Figure 3.3 for uniaxial, planar and biaxial extensions. The nonlinearity of the rubber stress–strain response can be observed, as well as the dependence on the mode of loading. The Yeoh model has been extensively used previously at Volvo and is also currently used by suppliers. It is often the material model of choice for filled rubbers (natural rubber used in engine mounts is always filled) as it has shown a good correlation to experimental data, especially at high strains. The material parameters C_{10} , C_{20} and C_{30} were obtained from work by Austrell [6], who compiled measurements for different rubber hardness. Engine mounts commonly vary in Shore hardness between 40 and 55, Austrell obtained Yeoh parameters for a few discrete hardness levels. Values in between were interpolated by polynomial interpolation, and are shown in Figure 3.4. A hardness of 45 was used throughout this investigation except when stated otherwise.

For comparison, the figure also shows the Yeoh parameters that were obtained from experimental data by Sandell [1] as part of a previous Master thesis at the Powertrain Mount division. These were not used in this project. The primary reason behind the discrepancy between the two is that the parameters from Sandell [1] were obtained in pure shear.

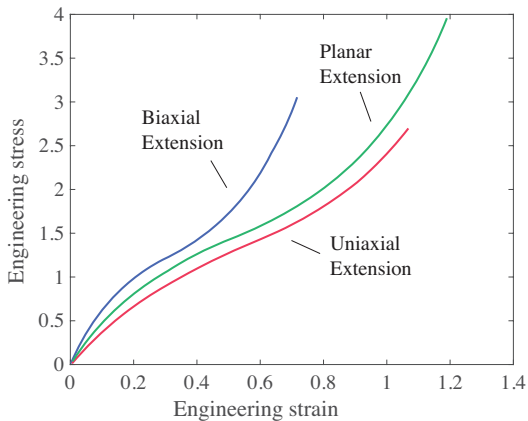


Figure 3.3: *The typical nonlinear behavior of rubber under different load cases.*

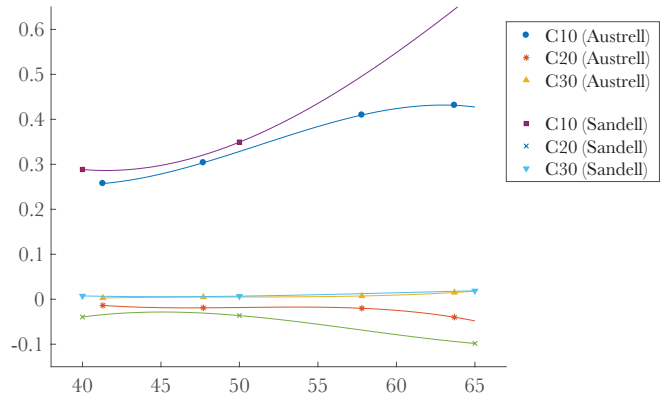


Figure 3.4: *Comparison between the Yeoh data of Austrell and Sandell.*

The operating temperatures of engine mounts and electric car mounts are around 110°C and 65°C, respectively. The change in stiffness of natural rubber compared to room temperature is negligible at these temperatures. In practice, material data at room temperature is used throughout the design phase. On the other hand, fatigue properties are greatly affected by a

change in temperature [20]. For this reason, fatigue tests are always performed at operating temperatures.

3.2 Numerical implementation of fatigue criteria

The theory behind the fatigue criteria were explained analytically in Chapter 2. These were implemented in Python using the NumPy library [31], as a plug-in to Abaqus/Viewer. The numerical implementations of these criteria are described in the following sections.

3.3 Peak maximum principal strain

The method was trivially implemented, as the maximum principal strain, $\varepsilon_{1,\max}$ is readily available in commercial FE software. The parameter consists of finding the peak value of the first (maximum) principal strain, ε_1 during fatigue cycle. If a fatigue cycle is discretized as the strain state going from point A to point B and back, or A–B–A, one can obtain the strain state at the two extremes, A and B, in a FE model. The reason the signal is converted into fatigue cycles is because the fatigue properties are described by a Wöhler relationship, which a criteria to the number of cycles, A–B–A, that the component can endure. The fatigue cycle is visualized in Figure 3.5.

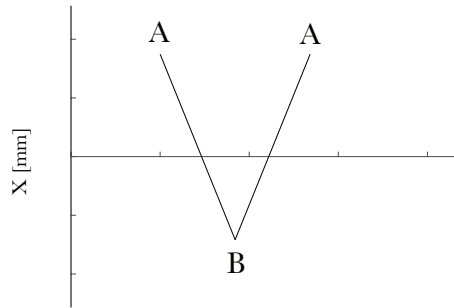


Figure 3.5: A fatigue load going from A, to B and back to A.

The peak principal strain during the cycle is then found as the maximum value of the two strain states:

$$\varepsilon_{1,\max} = \arg \max \{ \varepsilon_1^A, \varepsilon_1^B \} \quad (3.1)$$

In the numerical implementation, this peak is calculated for each fatigue cycle and the corresponding damage is obtained from a Wöhler relationship.

3.4 Cracking energy density

The cracking energy density is not as trivially implemented and is also computationally expensive. The method can be seen as associating the energy performed by the traction stress

on a plane (hypothetical crack surface). In other terms, the energy in this plane is the portion of energy available to be released on a certain plane [16]. The increase in energy density during a fatigue cycle is evaluated as

$$dW_c = t_i d\varepsilon_i \quad (3.2)$$

where $t_i = \sigma_{ij}r_j$ is the traction stress on the plane r_j and $d\varepsilon_i$ is the change in traction strain on the plane. This gives us more explicitly that

$$dW_c = r_j \sigma_{ij} d\varepsilon_{ik} r_k \quad (3.3)$$

For comparison, the commonly used strain energy density is calculated as

$$dW = \sigma_{ij} d\varepsilon_{ij} \quad (3.4)$$

As an assumption is made on the orientation of the crack, a finite number of evenly spaced orientations need to be checked, whereby after obtaining the energy at each orientation, the one with the maximum, $dW_{c,max}$, is defined as the orientation from which the crack is mostly likely to initiate. Figure 3.6 shows a half-sphere which visualizes the case of having 91 evenly spaced orientations.

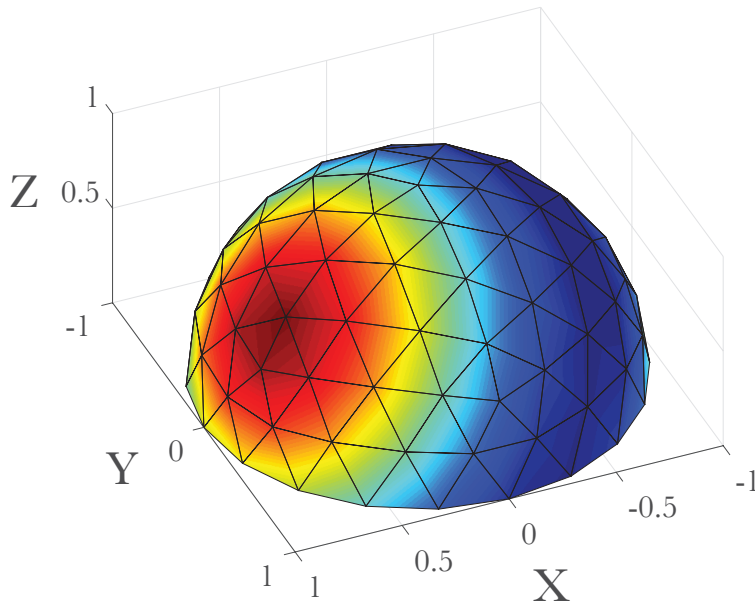


Figure 3.6: *Visual representation of the distribution of cracking energy density for different hypothetical cracking orientations.*

When calculating the damage from a load sequence, the damage obtained at each orientation and load cycle must be stored. The damage is then accumulated plane-wise until the sequence is completed. This is done simultaneously for all elements in the FE model. The orientation with the maximum accumulated damage defines the maximum damage of that element, as a crack can only initiate in one orientation.

The relationship in equation 3.2 is a simplification for fatigue under linear low-strain conditions without rotations of the nonlinear cracking energy density equation, which is only

valid. In order to capture the behavior of nonlinear deformation, which contains non-negligible rotations of the deformed body (in this case rotations of individual elements), *finite deformation theory* must be used.

For this reason, a description of W_c using finite deformation theory is required. This formulation should be able to handle changes when going from an undeformed to a deformed state. In particular, it must be able to translate the cracking plane orientations.

In finite deformation theory, one can refer to physical properties such as stress and strain in two ways, relative to the undeformed state, called the material description, or relative to the deformed state, the spatial description. In order to handle the nonlinearities that come with high strains, one must describe the cracking energy density in the spatial description in terms of the materials description.

The full derivation was done by Mars [16], by using the relationship between the (spatial) Cauchy stress $\boldsymbol{\sigma}$ and (material) 2nd Piola-Kirchhoff stress $\tilde{\boldsymbol{S}}$ (material) and the deformation gradient \boldsymbol{F} :

$$\boldsymbol{\sigma} = \frac{\rho}{\rho_0} \boldsymbol{F} \tilde{\boldsymbol{S}} \boldsymbol{F}^T \quad (3.5)$$

where ratio ρ/ρ_0 is the change in density from the undeformed to deformed state. The deformation gradient is defined as the derivative of each component of the deformed vector \boldsymbol{x} , with respect to each component in the undeformed vector \boldsymbol{X} :

$$\boldsymbol{F} = \frac{\partial \boldsymbol{x}}{\partial \boldsymbol{X}} \quad (3.6)$$

The strain is written in terms of the material description as

$$d\boldsymbol{\varepsilon} = \boldsymbol{F}^{-T} d\boldsymbol{E} \boldsymbol{F}^{-1} \quad (3.7)$$

which in total gives us the cracking energy density in terms of the material components as

$$dW_c = \underbrace{\boldsymbol{r}^T \left(\frac{\rho}{\rho_0} \boldsymbol{F} \tilde{\boldsymbol{S}} \boldsymbol{F}^T \right)}_{\text{Stress}} \underbrace{\left(\boldsymbol{F}^{-T} d\boldsymbol{E} \boldsymbol{F}^{-1} \right)}_{\text{Strain}} \boldsymbol{r} \quad (3.8)$$

The Cauchy stress $\boldsymbol{\sigma}$ is readily available in Abaqus, so calculating the first parenthesis in equation (3.8) is not required. The orientation vector \boldsymbol{r} is expressed in terms of the deformed configuration, but can be expressed in the undeformed configuration as

$$\boldsymbol{r} = \frac{\boldsymbol{F} \boldsymbol{R}}{|\boldsymbol{F} \boldsymbol{R}|} \quad (3.9)$$

where \boldsymbol{R} is the orientation vector in the undeformed configuration.

When calculating the change in CED, one wants the change from one deformed stress-strain state to another. From State 1 with the deformation and stress states \boldsymbol{F}_1 and $\boldsymbol{\sigma}_1$ to State 2 with \boldsymbol{F}_2 and $\boldsymbol{\sigma}_2$. The continuous change from the one state to the other is not known, so the change in energy must be approximated using the linear average of these two.

The average stress in (3.8) then becomes

$$\text{Average Stress} = \frac{1}{2} \left((\boldsymbol{r}^T \boldsymbol{\sigma})_2 + (\boldsymbol{r}^T \boldsymbol{\sigma})_1 \right) = \frac{1}{2} \left(\frac{\boldsymbol{R}^T \boldsymbol{F}_2^T}{|\boldsymbol{F}_2 \boldsymbol{R}|} \boldsymbol{\sigma}_2 + \frac{\boldsymbol{R}^T \boldsymbol{F}_1^T}{|\boldsymbol{F}_1 \boldsymbol{R}|} \boldsymbol{\sigma}_1 \right) \quad (3.10)$$

To obtain the strain part, the change in Green-Lagrange strain [16] is obtained as

$$d\mathbf{E} = \frac{1}{2} (d\mathbf{F}^T \mathbf{F} + \mathbf{F}^T d\mathbf{F}) \quad (3.11)$$

and a change in the deformation gradient is obtained from the fact that

$$\mathbf{F}_2 = d\mathbf{F} \mathbf{F}_1 \quad (3.12)$$

from which one gets

$$d\mathbf{F} = \mathbf{F}_2 \mathbf{F}_1^{-1} \quad (3.13)$$

which in discrete terms becomes

$$\Delta\mathbf{E} = \frac{1}{2} (\Delta\mathbf{F}^T \mathbf{F} + \mathbf{F}^T \Delta\mathbf{F}) = \left((\mathbf{F}_2 \mathbf{F}_1^{-1})^T \bar{\mathbf{F}} + \bar{\mathbf{F}}^T \mathbf{F}_2 \mathbf{F}_1^{-1} \right) \quad (3.14)$$

where $\bar{\mathbf{F}}$ is the mean of the two deformation gradients, i.e. $\bar{\mathbf{F}} = (\mathbf{F}_1 + \mathbf{F}_2) / 2$.

3.5 Fatigue failure criterion

It is important to have a well-defined criterion for fatigue failure. In metal fatigue, it is common to choose a crack size, a_f , at which failure is seen as imminent. This works well, as cracks in metal are often well defined and often an individual crack is the cause of structural failure in a component. However, this has turned out not to be a viable approach in practice when defining the failure of engine mounts, for two reasons: The function of engine mounts is to follow a specific force–displacement, or, for a specified displacement, a specified reaction force should be obtained (see Figure 2.6.) The second reason has to do with the fact that natural rubber often does not produce single well-defined cracks, but instead networks of ill-defined cracks are created which coalesce into larger damage zones [30]. For this reason, fatigue failure is defined as the point at which the static stiffness (the slope at the origin of the force–displacement curve) has reached below 20% of the original value. The value 20% has become a de facto value that is used throughout the automotive industry, although the author has not been able to find a source behind this choice.

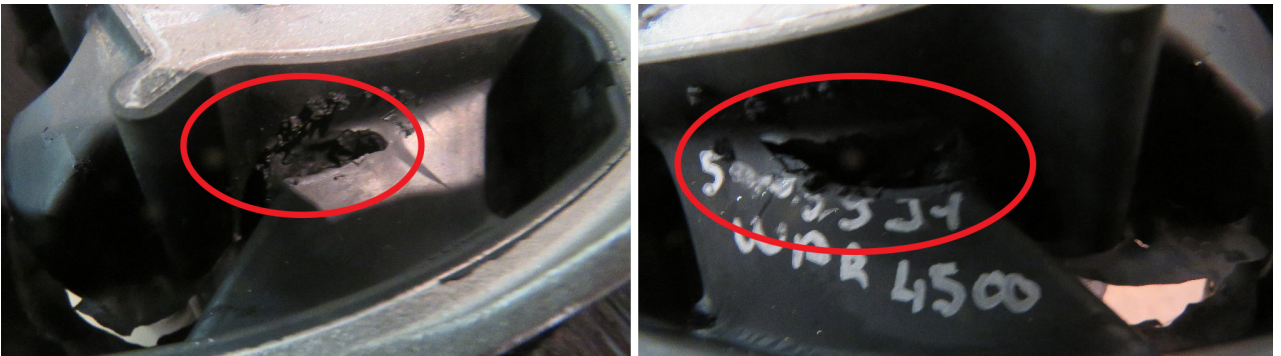


Figure 3.7: *Natural rubber is prone to causing networks of cracks that coalesce into a large defect. From [2].*

Figure 3.7 shows an engine mount that was subjected to a fatigue sequence. The missing mass in part of the MRE, highlighted in red, was caused by a network of cracks coalescing into one, which caused further damage to the MRE. For this reason, there is a poor correlation between crack size, which is often hard to define, and the static stiffness. The engine mount in question did in fact pass the fatigue test, having narrowly stayed above the 20% limit, as can be seen in Figure 3.8. It should be noted that the phenomenon of crack networks is much less prevalent in synthetic rubbers and crack size criteria are commonly deployed there.

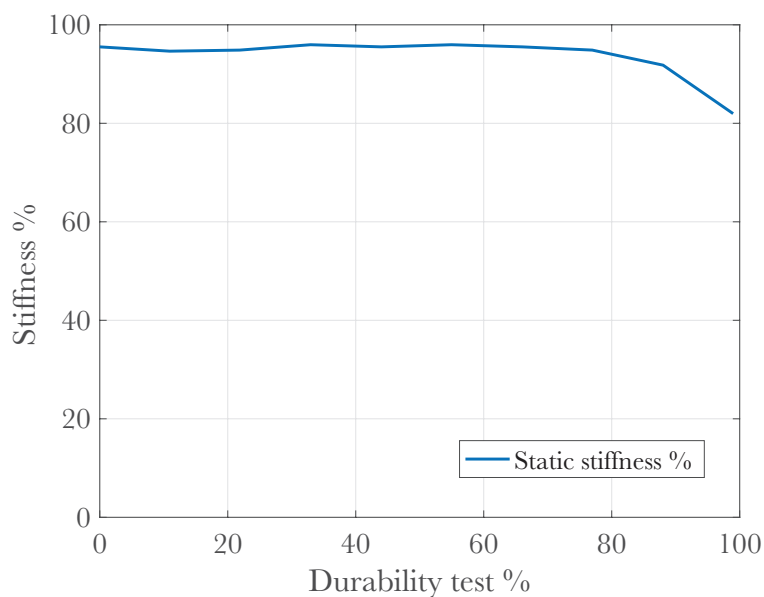


Figure 3.8: *At the end of the fatigue test, the static stiffness remained above 80%, and therefore passed the failure test [2].*

3.6 Constructing a fatigue relationship

The following describes the process of obtaining a Wöhler relationship by fatigue testing. This was outside of the scope of the thesis, and has therefore not been performed. This section serves as guidelines for future work as well as to provide completeness.

A Wöhler relationship is required to be able to predict fatigue life in engine mounts. This is obtained by loading several specimen at different constant-amplitude fatigue cycles. Figure 3.9 shows an example Wöhler curve obtained from 11 specimens.

It is important to perform all fatigue tests at the actual operating temperature, as fatigue life can vary by as much as a factor of 4 [20] if the temperature is varied. A cycle frequency must be chosen sufficiently high to reduce the total fatigue testing time, but also low enough to prevent excessive heat generation. One commonly chooses a frequency between 1–2 Hz. The tests at the lower end of the Wöhler curve, around the 10^7 – 10^8 range, can take up to a year to finish. It is therefore sensible to first perform the high-end fatigue tests (which take between a day to a week) in order to verify the fatigue setup before the longer tests are performed.

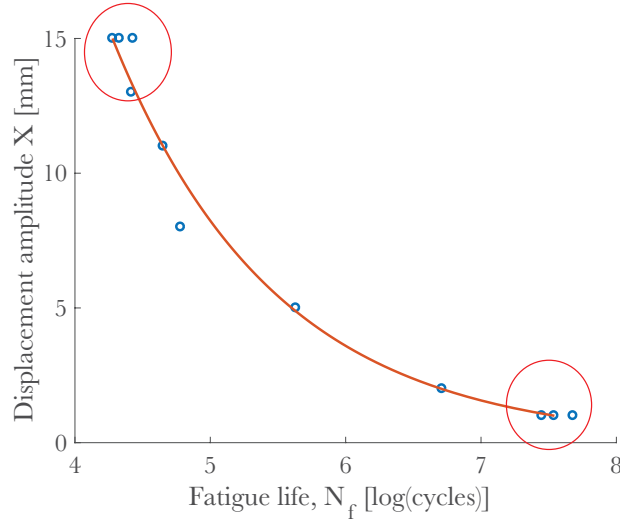
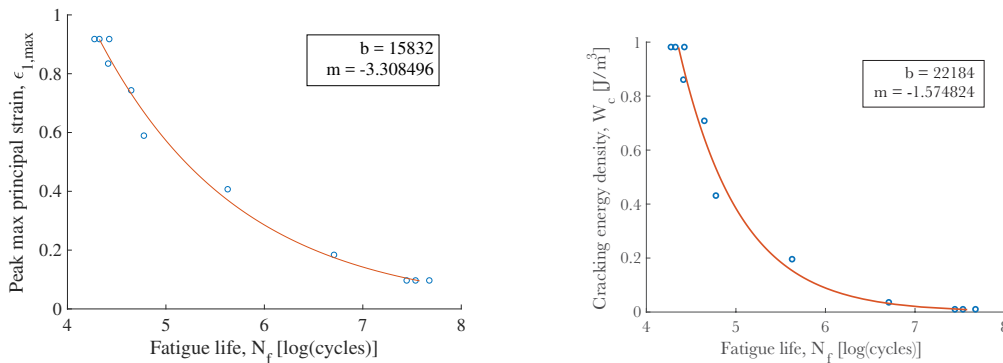


Figure 3.9: *Example of an exponential curve fitted to fatigue test data in order to obtain a Wöhler curve. The high-end and low-end amplitudes are highlighted in red.*

Ideally, one should perform several tests at each amplitude in order to establish the statistical variation of fatigue results to be used as a guideline for a safety factor. This is often not realistic because of time and specimen constraints. In such a case, one should try to perform at least 3 tests at the high-end amplitude and 3 tests at the low end, which will give a rough estimation of the statistical distribution.

Before fatigue testing can begin, one must determine the high-end and low-end amplitudes, which have been highlighted in red in Figure 3.9. The high-end amplitude should preferably be chosen close to the highest load magnitudes obtained from the lifetime load sequence. The low-end amplitude should optimally be chosen based on the lowest load magnitudes in the compressed lifetime load sequence. This allows for the low-end amplitude not to be too low, lessening the total time required to obtain the full Wöhler curve.

The Wöhler curve in Figure 3.9 is a relationship between the displacement amplitude and the fatigue life. In order to make it applicable for other geometries, materials and to some extent, nonzero mean stresses and strains, one wishes to convert the Amplitude- N_f relationship into a $\epsilon_{1,\max}$ - N_f or a W_c - N_f relationship, as shown in Figure 3.10.



(a) *The Wöhler curve as a relationship between the peak principal strain and number of cycles.*

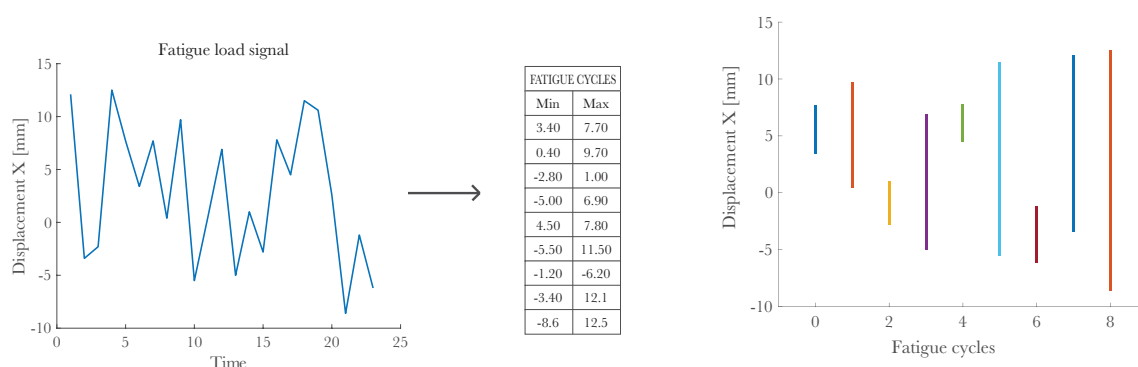
(b) *The Wöhler curve as a relationship between CED and number of cycles*

Figure 3.10: *Two Wöhler curves for the same fatigue testing data.*

For this to be done, each cycle amplitude is simulated in an FE analysis. For each amplitude, the corresponding peak principal strain or CED is calculated. One then obtains the much more useful relationships, shown for both parameters in Figure 3.10. These are used to predict the fatigue life of the component during its lifetime.

3.7 Fatigue life prediction: Variable-amplitude loading

The fatigue life of a component is represented as the damage distribution of the component. If at any point in time and space the damage is above 1, the component is considered to have experienced fatigue failure. One must convert a lifetime load sequence obtained from data from test track drives or dynamic rigid body simulations into a sequence of fatigue cycles, such as the one shown in Figure 3.11.



(a) The load sequence and corresponding fatigue cycles.

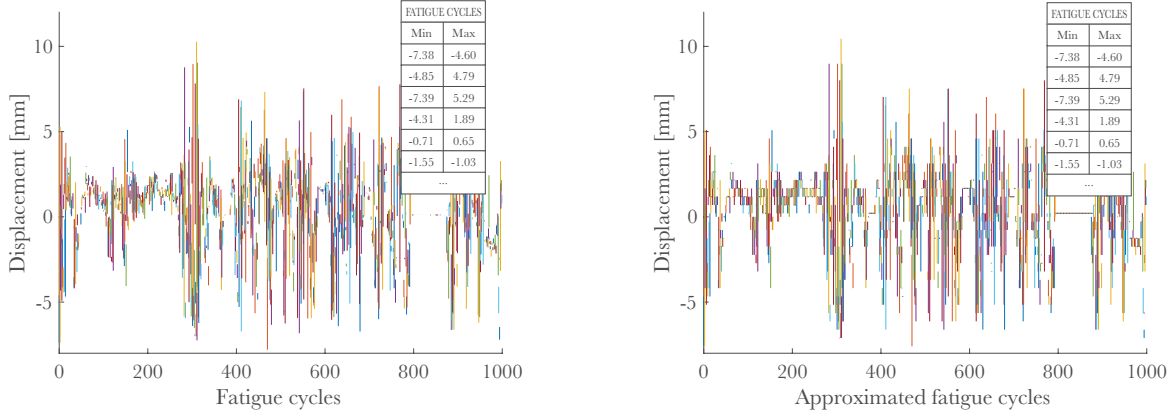
(b) The fatigue cycles visualized.

Figure 3.11: a) The load sequence is converted into fatigue cycles using rainflow counting. b) The cycles can be visualized in the figure to the right.

This is commonly achieved using the so-called *rainflow counting* [32] algorithm. The algorithm is not explained here, but a simple example of a load sequence which was converted into fatigue cycles.

In order to calculate the peak principal strain or CED, which are functions of the stress–strain state, the FE analysis must be carried out at each unique minimum and maximum point of every fatigue cycle. A lifetime load sequence, such as in Figure 3.12 a), commonly contains millions of unique fatigue cycles and it would be unfeasible to obtain the stress–strain state for each of these through FE analyses. This is solved by limiting the two ends of the fatigue cycles to a set of predefined values. The minimum and maximum values of the fatigue cycle are approximated to the nearest value in the predefined set. For example, if a set of 50 linearly distributed values are chosen, ranging from the minimum to maximum value in the full sequence, the resulting "approximated" sequence of fatigue cycles would become as shown in Figure 3.12 b). The number of predefined values that are chosen could be seen as the *resolution* of the fatigue cycle sequence. It is important to find a sufficiently high resolution, as it will affect the accuracy of the fatigue life prediction results, while keeping computational resources in mind. The effect on the choice of resolution is assessed later.

The total damage distribution in the model can now be calculated by obtaining either the peak principal strain or CED parameter in each element (in practice, in each integration point)



(a) The original fatigue cycles make up millions of unique values.

(b) The approximated fatigue cycles have only 50 values to choose from, as such the cycles have a resolution of 50.

Figure 3.12: The original fatigue cycles in a) get approximated to the cycles shown in b).

for each fatigue cycle. For each cycle, the fatigue life is related to the Wöhler curve power law

$$N_f = bA^m \quad (3.15)$$

where A is a fatigue criterion. The damage is defined as $D = 1/N_f$ and the cumulative damage for each element is obtained from Miner's rule:

$$D_{\text{tot}} = \sum_{i=1}^N N_{f,i} = \frac{1}{N_{f,1}} + \frac{1}{N_{f,2}} + \dots + \frac{1}{N_{f,N}} \quad (3.16)$$

The total damage distribution, as a result of the lifetime load sequence, is finally obtained. Figure 3.13 demonstrates such a damage distribution.

In summary, one has a load sequence that represents the lifetime loading of a component, which is converted into fatigue cycles. These fatigue cycles are approximated by binning their minimum and maximum values into a set of finite values, in order to make FE modeling feasible. From the stress and strain state of each fatigue cycle, the fatigue damage is calculated from the Wöhler relationship in equation 3.15 and are summed up with equation 3.16. The total damage distribution indicates if any point on the component will cause fatigue failure during the component lifetime.

3.8 Physical load sequence testing (verification of fatigue life predictions)

Once a geometry has been established that satisfies the durability requirements according to fatigue life prediction results, one must verify the prediction results by physical testing of the component. The component should be subjected to the same load sequence that was used in the fatigue life prediction process. However, as these signals consist of millions of signal points, the load sequence must be compressed. This is done by removing negligible load fluctuations

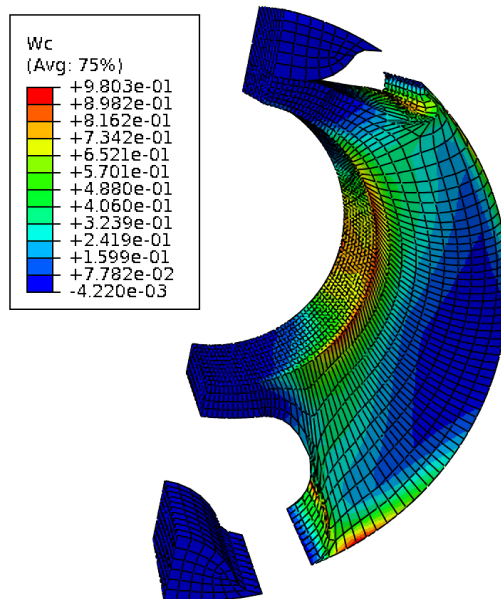


Figure 3.13: *The damage distribution of a bushing subjected to the load sequence above. The damage is concentrated to where the rubber connects to the aluminum, as expected.*

and insignificant smaller loads, in order to be able to carry out the physical tests within a reasonable amount of time.

For an engine mount, the lifetime load sequence is defined by a number of *events*, such as:

- Event 1: Full throttle, 0-70 kmh, engine break, $\times 10,000$
- Event 2: Reversal up 16% slope (no wheel slip), $\times 900$
- Event 3: Cobblestone cornering 25 kmh, $\times 3400$
- ...

Each event is repeated a specified number of times, which makes up the lifetime load sequence. If one were to subject a physical component to this full load sequence, it would take approximately 11 weeks, which would severely affect development lead times. Instead, one aims at a testing sequence of a few days at most. This means that the load sequence must be compressed. Determining the extent to which the signal can be compressed is best done by comparative physical testing, but in lieu of expensive testing, it can also be performed by simulations. The load sequence is compressed with different intensities, rainflow counting is performed and one obtains the total damage as a function of the amount of load sequence compression and is able to decide the allowable magnitude of signal compression.

3.9 The rubber fatigue toolset

The process which has so far been described in Chapter 3 was implemented and compiled into a toolset. A preprocessor was implemented in MATLAB for processing of a load sequence,

with rainflow counting and generation of Abaqus *STEP commands. A postprocessor Abaqus plug-in for calculating the damage distribution using either the peak principal strain or CED was written in Python. A post-processor for curve fitting Wöhler curves to a power law was also developed in MATLAB. The toolset enables:

- Fatigue testing where the relationship between peak principal strain and CED and the number of cycles until failure is obtained.
- Curve fitting to a power law bA^m and plotting of a Wöhler curve.
- Evaluation of the sensitivity to choice of fatigue cycle resolution.
- Evaluation of allowable load signal compression for physical testing.
- Fatigue life prediction by damage distribution of a component subjected to a loading sequence.

is increased, and as such the change in fatigue life. This is because CED takes into account both the stress and strain. A harder rubber, subjected to the same displacement-controlled loading, produces higher stresses, and in turn a shorter fatigue life. It should be noted that in this uniaxial case, because the cracking plane of highest W_c is parallel to the Cartesian coordinates, the strain energy density would produce the same results as cracking energy density.

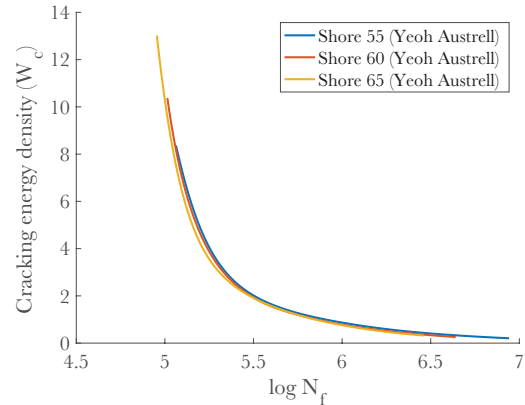
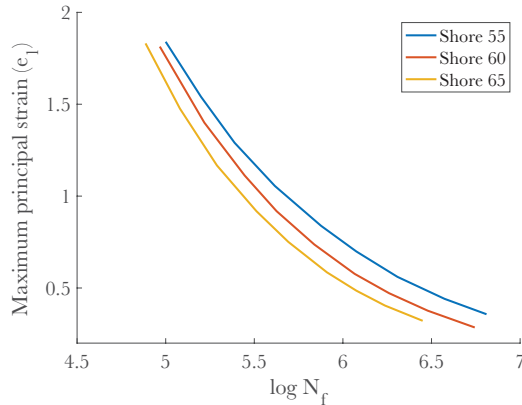


Figure 4.2: *One obtains a different Wöhler curve for each hardness when using the peak dependent of hardness principal strain.*

In conclusion, the cracking energy density is a more viable fatigue criteria if one wishes to change the rubber hardness while keeping the same Wöhler relationship.

Another article by Woo [22], the same dumbbell geometry was subjected to fatigue testing at varying mean displacements. It can be seen how an increase in mean displacement leads to a worse fatigue life. The fatigue loads were evaluated in Abaqus and calculated with respect to the maximum principal strain, shown in Figure 4.4. The principal strain is able to capture the effect of the mean displacement fairly well, however, the ends of the curves diverge and this divergence becomes worse with increasing difference in mean displacement. For example, between the 0 mean and 3 mean curves, the fatigue goes from $10^{7.3}$ to $10^{6.9}$, a loss of 60% of the fatigue life. This is caused by two things: The power law, which each curve was constructed from, is not optimal in describing the fatigue life. This is because of the nonlinearities of rubber fatigue, especially in this case the nonlinear stress-strain response. The second reason is that higher mean displacements in natural rubber results in effects such as strain crystallization, which alters the microstructure of the rubber. There is no established method of mean strain correction in rubber fatigue, likely given the relatively good correlation by simply using the peak maximum principal strain. The fatigue tests were evaluated in Abaqus and the cracking energy density was calculated, shown in Figure 4.5.

Generally, the cracking energy density yields somewhat of a better fit, especially at the lower fatigue lives. It is not markedly better however, and in practice there would likely not be much of a benefit in using CED over the principal strain in terms of correcting for mean displacement. It should be noted that mean strain is usually not accounted for in the industry when prediction fatigue life of engine mounts.

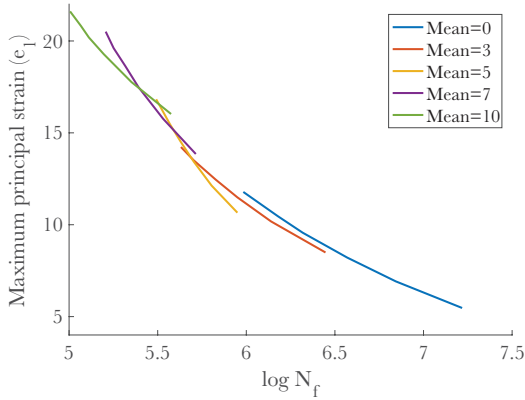


Figure 4.4: *The Wöhler curve using the peak principal strain.*

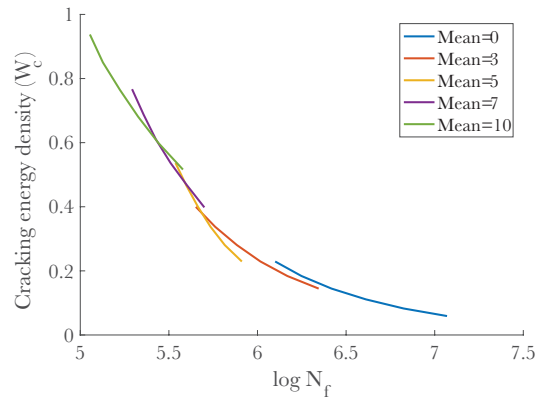


Figure 4.5: *The Wöhler curve using the cracking energy density.*

4.2 Sensitivity to evaluated crack orientations

An FE model was created with the purpose of providing a stress-strain response similar to the MREs in an engine mount. The model is shown in Figure 4.6 with a width of 76 mm and an element size of 2 mm. The objective was to examine the sensitivity of evaluated CED magnitudes with respect to the number of crack orientations and fatigue cycle resolution.

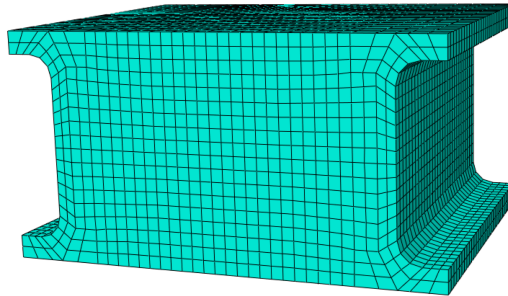


Figure 4.6: *The shear block used for evaluating the crack orientation sensitivity.*

The model was tested by a lifetime load sequence currently in use for evaluating engine mounts. The signal is equivalent to road conditions experienced by a mount during the lifetime of the component. The dependence on the number of cracking energy density orientations was of interest. To this end, several sets of orientation vectors were generated. With the purpose of checking orientation planes at equal increments, the nodes from a set of icosahedra were used as the orientations of the normal vectors. The smallest possible icosahedron has 26 nodes. The faces of the icosahedron were subdivided into successively smaller triangles which generated more orientations. Figure 4.7 shows three icosahedra with 26, 196 and 526 nodes, respectively.

For each set of cracking orientations, the total predicted damage is plotted as shown in Figure 4.8. It can be observed that the percentage in error (compared the overkill of 526 angles) of the total damage does converge. A good compromise between accuracy and required memory is found when using 91 orientations, which corresponds to an error of approximately 1%. It

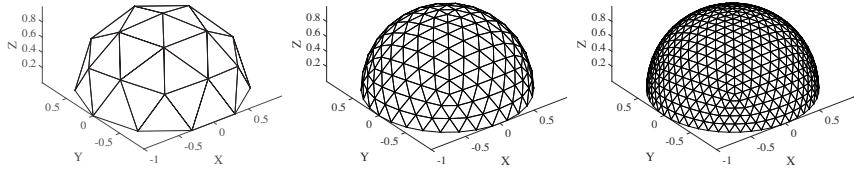


Figure 4.7: Three icosahedra with 26, 196 and 526 nodes respectively.

should be noted that more complex geometries and load cases may require more orientations to be used. However, engine mounts are at most loaded in two modes at once: tensile and shear. Under such conditions, 91 or 196 orientations should suffice, according to the results.

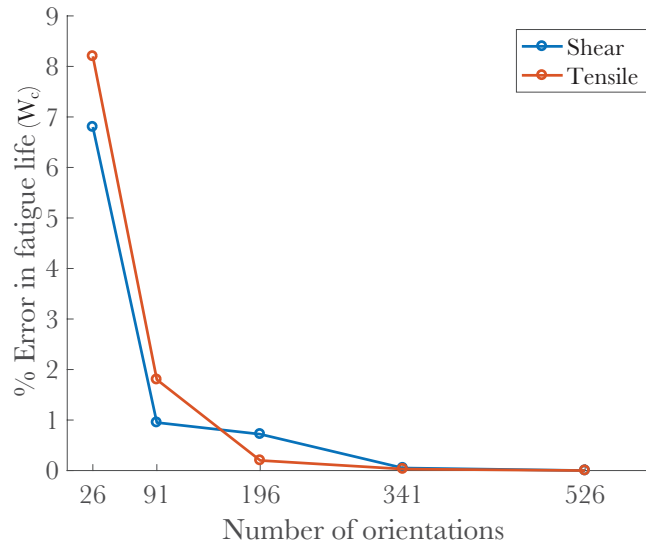


Figure 4.8: The error can be seen to converge as the number of crack orientations increases.

4.3 Sensitivity to fatigue cycle resolution

A bushing, based on the bushing geometry presented in [33], is shown in Figure 4.10. The bushing was examined to evaluate the sensitivity with respect the resolution in the fatigue cycles (see Figure 3.12.) Figure 4.9 shows the error in total damage as a function of fatigue cycle resolution as well as execution time. The error can be see to converge rather quickly, which could be explained by the way fatigue cycles are approximated. When the fatigue cycles are rounded to the nearest value in the predefined set of minimum and maximum fatigue cycle values, one may assume that it is statistically probably that an equal amount of fatigue cycles get overvalued and undervalued. This means a lower resolution of the fatigue cycles still gives a good approximation when the damage of all cycles are summed up. Although the overvalued

and undervalued cycles would not completely cancel out, as the Wöhler curve is not a linear relationship, the effect appears to be sufficiently large to lead to a quick convergence in error magnitudes. It should be noted that only a portion of the load sequence. The actual execution time for the entire load sequence would total a few hours, which may motivate a lower fatigue cycle resolution.

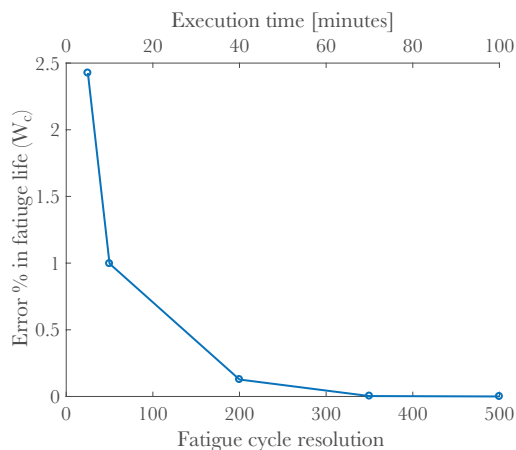


Figure 4.9: The error is shown with respect to the resolution of the fatigue cycles.

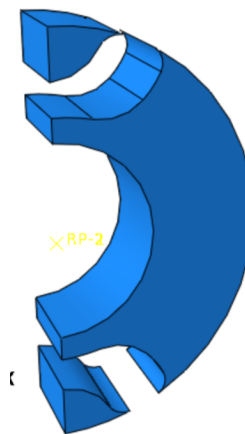


Figure 4.10: The bushing (symmetric) evaluated to establish sensitivity to fatigue cycle resolution and fatigue cycle reduction.

4.4 Sensitivity to removal of fatigue cycles

The same bushing was evaluated for the sensitivity to the removal of the smallest fatigue cycles when using CED. The evaluation was done at a fatigue cycle resolution of 50. The fatigue cycles were removed based on their range, under the assumption that a greater range would produce a greater CED. The purpose of removing fatigue cycles is to reduce the execution time, and therefore was therefore performed during the preprocessing stage, where the fatigue cycles are defined by the displacement. The displacement range of each cycle is compared to the highest range in the sequence and is removed if it is below a certain threshold. For example, if a 25% cutoff threshold is chosen, all cycles with a range of 25% or less than that of the cycle with the greatest range are removed. Figure 4.11 shows a set of fatigue cycles, where the fatigue cycles whose range is 25% or less are crossed out (and thus would be removed.) Figure 4.12 shows the result of fatigue cycle removal of the bushing, but as can be seen, the error increases quickly, with little benefit to execution time. As such, removing the smallest fatigue cycles in order to reduce the execution time is of no advantage compared to the loss of accuracy, according to the results.

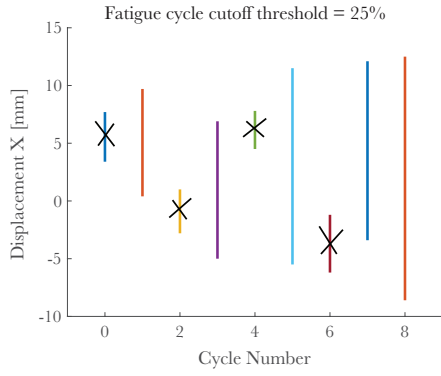


Figure 4.11: *The fatigue cycles whose displacement range is less than 25% of the greatest range are removed.*

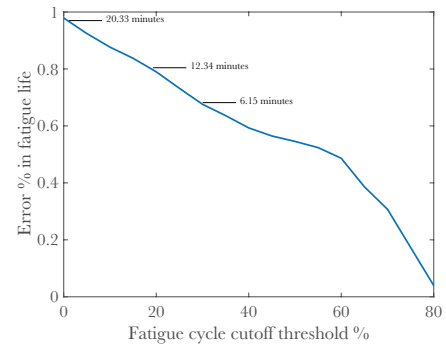


Figure 4.12: *The error increases rapidly with increasing removal of small fatigue cycles, without any benefit in execution time.*

5 Discussion and conclusions

5.1 Discussion

Understanding and implementing fatigue life prediction models for rubber required knowledge of several disciplines. Fatigue theory of rubber is adopted from the finding and conjectures of the mature field of metal fatigue, but simplifications that are viable in metal fatigue are not possible with natural rubbers. For rubbers, both the material response and the geometric displacements are nonlinear at loads at which fatigue becomes relevant. Even worse, there seems to be no generalized theory of fatigue of natural rubbers available. This means that fatigue life testing must be performed on a component basis.

The thesis focused on two fatigue criteria that are in stark contrast to each other: the maximum principal strain is the most rudimentary method of fatigue evaluation and is easily evaluated from FE simulation results. In contrast, the only other method that has shown any significant improvement in results is the cracking energy density, which require an expensive post-processing that can easily take longer than the FE simulations from which the stresses and strains are obtained.

At the beginning of the thesis work, the commercial software fe-safe/Rubber seemed like a good candidate for verifying the in-house implementation of the two fatigue criteria. It was even considered as the primary rubber fatigue tool in case the in-house methods would have failed to give adequate results. However, early on in the project it was realized that the software database lacked the appropriate natural rubbers used in engine mounts. These are in the range of 40–55 in Shore hardness. Further the software was generally focused on synthetic rubbers. Additionally, the fatigue predictions were based on theory behind the software use of the principle of the crack failure length. As discussed in this report, this does not correlate well with the loss of function of an engine mount made from natural rubber. The use of a critical crack length as a fracture criterion may explain the lack of natural rubbers and the abundance of synthetic rubbers in the material database, in contrast to natural rubbers, as synthetic rubbers tend to have single well-defined cracks.

Obtaining fatigue data for rubber components is an investment in capital, but even more in time. When first establishing a fatigue relationship, the components that are subjected to the lowest loads do not fail until after around 10^7 load cycles. The test frequency is limited by the heat generation from the internal friction, as the temperature must stay within a narrow window at engine mount operating temperatures in order not to affect the fatigue results. Letting the engine mount heat itself up by cyclic loading at a high frequency would also not work, as rubber has a low conductivity of heat and one would end up with a temperature gradient. For this reason one cannot avoid long fatigue testing times.

Given the lack of fatigue data of engine mounts available for the thesis work, the results focused on sensitivity studies. The results seem to suggest that in the engine mount hardness range, the cracking energy density was better correlated to fatigue life as the rubber hardness is changed. The study was however performed on dumbbell specimen. No studies on engine mounts of varying hardness have been carried out.

The comparisons between the peak principal strain and CED, choice of number of crack orientations, fatigue cycle resolution and cycle removal serve as guidelines for in-house fatigue life prediction of engine mounts, which was the motivation behind the thesis work. The results are easy to reproduce using the toolset that was developed during the course of the project. It

should be stressed again that when performing fatigue life predictions with FE models, it is important to stay consistent in terms of mesh, material properties, boundary conditions and load conditions, and it is necessary to document all details and procedures well, especially considering the long time scales that are involved in fatigue evaluation.

A mesh convergence study was not performed on an engine mount because of three reasons. Meshing of engine mounts is complex and creating increasingly finer mesh refinements is difficult, as the large deformations cause element distortions that are hard to predict. What one ends up doing in order to get the nonlinear FE models to converge is to finely control the element distribution of each corner and fillet. As such, meshing an engine mount can take several hours. One therefore generally uses a single finely meshed model when performing FE analysis. Given this is a limitation that is experienced through all of the automotive industry, where fatigue life prediction is already successfully performed using both the peak principal strain and the cracking energy density, the use of mesh that is as fine as possible should suffice.

5.2 Conclusions

From the thesis work it was concluded that:

- Fatigue life prediction of engine mounts in the industry should be made on a component basis.
- The fatigue software fe-safe/Rubber is not sensible for fatigue life prediction of engine mounts for the reasons discussed in the report.
- The peak principal strain and cracking energy density are (currently) the two sensible fatigue evaluation criteria to use. The first is easy to calculate and good for initial estimates, the second is resource-intensive but provides better results.
- Fatigue testing needs to be performed in order to obtain a Wöhler relationship. However, once it has been obtained, the relationship can be used for subsequent designs.
- The results on the influence of various parameters such as the fatigue cycle resolution should be used as guidelines for obtaining accurate fatigue life prediction results.

5.3 Recommendations and future work

It is recommended that fatigue testing be performed on the engine bushing designs were the basis for the thesis work. The fatigue evaluation toolset was developed to be easy to understand, and therefore enable further development. The accuracy of the toolset will be fully evaluated once fatigue results have been obtained. It is recommended that the sensitivity studies that were done in the work are reproduced on the final bushing design. That in-house fatigue evaluation is possible has been shown. However, the level of accuracy that can be obtained remains to be seen.

References

- [1] V. Sandell. Extraction of material parameters for static and dynamic modeling of carbon black filled natural rubbers. *Luleå University of Technology* Master thesis (2017).
- [2] V. C. Corporation. *Volvo cars in brief*. 2016.
- [3] Python Software Foundation. *Python Language Reference, Version 2.7*, Accessed February 5, 2018. <https://www.python.org>.
- [4] The MathWorks Inc. *MATLAB, Version 8.6.0.267246 (R2015b)*, Accessed February 5, 2018. <https://www.mathworks.com>.
- [5] Dassault Systèmes. *Abaqus/CAE, Version 6.14*, Accessed March 31, 2017. <https://www.3ds.com>.
- [6] P. E. Austrell. *Modeling of elasticity and damping for filled elastomers*. Report, TVSM-1009. Lund University, 1997.
- [7] R. Öhrn. Prediction of static and dynamic behavior of powertrain suspension rubber components. *Linköping University* Master thesis (2015).
- [8] J. Medbo. Method for structural optimization of powertrain mounts. *Chalmers University of Technology* Master thesis (2016).
- [9] W. V. Mars. A literature survey on fatigue analysis approaches for rubber. *International Journal of Fatigue* **24** (2002), 949–961. DOI: 10.1016/S0142-1123(02)00008-7.
- [10] A. K. Olsson. *Finite element procedures in modeling the dynamic properties of rubber*. Doctoral Thesis. Lund University, 2007.
- [11] W. D. Kim et al. Fatigue life estimation of an engine rubber mount. *International Journal of Fatigue* **26** (2003), 553–560.
- [12] K. M. Schmoller and A. R. Bausch. Similar nonlinear mechanical responses in hard and soft materials. *Nature Materials* **12** (2013), 278. DOI: 10.1038/nmat3603.
- [13] C. B. Bucknall, C. P. Buckley, and N. G. McCrum. *Principles of Polymer Engineering*. Oxford University Press, 1997.
- [14] M. J. Wang. The role of filler networking in dynamic properties of filled rubber. *Rubber chemistry and technology* **72(2)** (1999), 430–448. DOI: 10.1038/nmat3603.
- [15] Y. Yin et al. Effect of nucleating agents on the strain-induced crystallization of poly(l-lactide). *Polymer* **65** (2013), 223–232. DOI: 10.1016/j.polymer.2015.03.061.
- [16] W. V. Mars. Chapter 7 – Heuristic approach for approximating energy release rates of small cracks under finite strain, multiaxial loading. *Elastomers and Components* (2006), 91–111. DOI: 10.1533/9781845691134.1.91.
- [17] W. V. Mars and A. Fatemi. Nucleation and growth of small fatigue cracks in filled natural rubber under multiaxial loading. *Journal of Materials Science* **41** (22 2006), 7324–7332. DOI: 10.1007/s10853-006-0962-2.
- [18] A. Wöhler. Wöhler’s experiments on the strength of metals. *Engineering* **2:160** (1867).
- [19] S. M. Cadwell et al. Dynamic fatigue of life of rubber. *Industrial and Engineering Chemistry, Analytical Edition* **12** (1940), 19–23. DOI: 10.1021/ac50141a006.
- [20] X. Duan et al. The mechanical fatigue limit for rubber. *Journal of Automotive Engineering* **230** (7 2015), 942–954. DOI: 10.1177/0954407015597795.
- [21] G. J. Lake and P. B. Lindley. The mechanical fatigue limit for rubber. *Journal of Applied Polymer Science* **9** (1233 1965), 51.

- [22] C. S. Woo and W. D. Kim. Fatigue lifetime prediction methodology of rubber components. *High Performance Structures and Materials* **97** (IV 2008), 285. DOI: doi:10.2495/HPSM080301.
- [23] C. S. Woo and W. D. Kim. Fatigue life prediction of heat-aging vulcanized natural rubber. *Key Engineering Materials* **321-323** (2006), 518–521. DOI: 10.4028/www.scientific.net/KEM.321-323.518.
- [24] W. V. Mars and A. Fatemi. Multiaxial fatigue of rubber: Part I: equivalence criteria and theoretical aspects. *Fatigue & Fracture of Engineering Materials & Structures* **28** (2005), 515–522. DOI: 10.1111/j.1460-2695.2005.00891.x.
- [25] A. G. Thomas. Rupture of rubber. V. Cut growth in natural rubber vulcanizates. *Journal of Polymer Science* **31.123** (1958), 467–480. DOI: 10.1002/pol.1958.1203112324.
- [26] H. W. Greensmith. Rupture of rubber. X. The change in stored energy on making a small cut in a test piece held in simple extension. *Journal of Polymer Science* **7** (1963), 993–1002.
- [27] P. B. Lindley. Energy for crack growth in model rubber components. *Journal of Strain Analysis* **7** (132 1972), 40.
- [28] T. W. Kim et al. Prediction of the fatigue life of tires using CED and VCCT. *Key Engineering Materials* **297-300** (2005), 102–107. DOI: 10.4028/www.scientific.net/KEM.297-300.102.
- [29] W. V. Mars. Multiaxial fatigue crack initiation in rubber. *Tire Science and Technology* **29.3** (2001), 171–185. DOI: 10.2346/1.2139510.
- [30] R. Harbour, A. Fatemi, and W. Mars. Fatigue life analysis and predictions for NR and SBR under variable amplitude and multiaxial loading conditions. *International Journal of Fatigue* **30** (2008), 1231–1247. DOI: 10.1016/j.ijfatigue.2007.08.015.
- [31] The Scipy Community. *NumPy Reference, Version 1.14, Accessed February 10, 2018.* <https://scipy.org>.
- [32] S. D. Dowling and D. F. Socie. Simple rainflow algorithm. *International Journal of Fatigue* **4** (1982), 31–40.
- [33] B. Z. Q. Li J.-c. Zhao. Fatigue life prediction of a rubber mount based on test of material properties and finite element analysis. *Engineering Failure Analysis* **16** (2009), 2304–2310.
- [34] H. S. Ro. Modeling and interpretation of fatigue failure initiation in rubber related to pneumatic tires. *Multibody System Dynamics* Ph.D. Dissertation (1989).
- [35] C. L. Chow and T. J. Lu. Fatigue crack propagation in metals and polymers with a unified formulation. *Tire Science and Technology* **20.106** (1992), 29. DOI: 10.2346/1.2139510.
- [36] C. L. Chow and T. J. Lu. On the cyclic J-integral applied to fatigue cracking. *International Journal of Fracture* **40.52** (1989), 9. DOI: 10.2346/1.2139510.
- [37] R. J. Harbour, A. Fatemi, and W. V. Mars. Fatigue crack growth of filled rubber under constant and variable amplitude loading conditions. *Fatigue & Fracture of Engineering Materials & Structures* **30** (2007), 640–652. DOI: 10.1111/j.1460-2695.2007.01143.x.
- [38] A. Zine et al. Prediction of rubber fatigue life under multiaxial loading. *Fatigue & Fracture of Engineering Materials & Structures* **29** (2006), 267–278. DOI: 10.1111/j.1460-2695.2005.00989.x.
- [39] N. Saintier, G. Cailletaud, and R. Piques. Fatigue life prediction of natural rubber components under uniaxial and multiaxial loading. *Centre des mat eriaux P M FOURT* (2006), Ecole Nationale Sup erieure des Mines de Paris.

- [40] A. N. Gent and C. Wang. Fracture mechanics and cavitation in rubber-like solids. *Journal of Materials Science* **26** (1991), 3392–3395.
- [41] J. G. R. Kingston and A. H. Muhr. Determination of effective flaw size for fatigue life prediction. *Constitutive Models for Rubber VII* (2012).
- [42] G. Ayoub et al. Fatigue Life Prediction of Heat-Aging Vulcanized Natural Rubber. *International Journal of Solids and Structures* **48** (2011), 2458–2466. DOI: 10.1016/j.ijsolstr.2011.04.003.
- [43] Endurica. *fe-safe/Rubber*, Accessed February 5, 2018. <https://www.3ds.com>.